

# Preliminary development of optical fiber sensors numerical models for aerospace systems monitoring

ALESSANDRO AIMASSO, MATTEO BERTONE, PAOLO MAGGIORE,  
MATTEO D. L. DALLA VEDOVA  
Department of Mechanical and Aerospace Engineering  
Politecnico di Torino  
C.so Duca degli Abruzzi 24, 10129, Torino  
ITALY

**Abstract:** - The development of cutting-edge innovative systems in the mechanical and aerospace sectors firstly requires the use of a versatile and integrated sensor network. This approach allows to measure various physical parameters with the same hardware, thus generating smart components: optical fiber sensors are particularly suited for this purpose due to their physical characteristics. On the other hand, it is also essential to develop models that can accurately reproduce the physical behavior of the system. However, in the case of smart components equipped with optical fiber sensors, it is also necessary to model the response these sensors provide. This method can guarantee specific benefits, such as virtual sensing or decoupling the effects acting on the same sensor. This article considers the thermal and mechanical effects acting on a Fiber Bragg Grating sensor. A first-order model was employed for the thermal case, and a second-order mass-spring-damper model was used for the mechanical case. Finally, the numerical results were compared with the physical system, highlighting the good accuracy of the proposed approach and possible future developments.

**Key-Words:** - Aerospace Systems, Optical Fiber, Sensors, Models, Digital twins, Dynamic tests, Smart Systems.

Received: April 9, 2024. Revised: August 23, 2024. Accepted: September 27, 2024. Published: October 17, 2024.

## 1 Introduction

In the field of mechanical systems engineering, the measurement and monitoring of specific physical parameters play a crucial role, especially for components related to safety-critical applications [1]. One of the most advanced aspects in this regard is the possibility of developing *smart systems*: this means having the ability to integrate a minimally invasive network of sensors, either during the production phase of the components or applicable to an already completed system. Additionally, a particularly significant aspect is the possibility to measure very different physical parameters, such as temperature, strain, pressure or humidity, using the same hardware; thus generating large amounts of data to be processed through specific control logics. These algorithms can ensure a wide range of systems engineering applications, moving from real-time monitoring to Fault Detection and Identification (FDI) system, or Prognostic and Health Management (PHM) activities. Furthermore, for various industrial applications and specifically for aerospace, it is essential that the sensor network should guarantee high performance while operating in a hostile environment. The research activity described in this paper, involves the use of Fiber Bragg Grating (FBG)

optical fiber sensors for monitoring aerospace systems [2]. Fiber optic technology, indeed, is well suited to the aerospace sector, particularly thanks to its unique physical characteristics, such as minimal invasiveness, electrical passivity, and immunity to electromagnetic disturbances. While it can be said that fiber optics is a well-established technology for communication and data transmission, it has only recently begun to be used for sensor applications. In fact, in addition to maintaining the aforementioned advantages, it can combine high sensitivity to key physical parameters while working in harsh environments [3-10]. Simultaneously, numerical modeling is fundamental in the design and management of typical aerospace (or mechanical) engineering systems [11-12]. Therefore, considering the probable increasingly use of fiber optic sensors in systems of various kinds, to pursue the ambition to generate *smart components* and *smart systems*, - it has begun crucial to provide a possible modeling of their response. This process appears even more relevant considering their cross sensitivity to different physical parameters simultaneously and their extreme sensitivity to the boundary conditions to which the fiber optic is exposed. The purpose of this paper is therefore to provide a preliminary

application of first and second-order models, in order to numerically calculate the response of a generic FBG sensor. In particular, in this work different models are considered to reproduce the sensor response to both first-order thermal transients and second-order mechanical ones. The results are then compared to the response of real sensors, measured through a specific test campaign, in order to verify the validity of the proposed model and the adopted parameters. If appropriately developed and expanded, it is believed that modeling the response of an FBG optical sensor can provide an essential digital twin for future applications of this technology in different systems for prognostic and diagnostic.

## 2 Optical fibers

The operating principle of optical fiber lies in its ability to conduct a light beam within it. If light is correctly introduced into the core of the fiber, when it reaches the interface with the cladding, it undergoes total internal reflection, thus remaining confined within the core and propagating the information along the fiber itself. From a section of optical fiber, it's possible to obtain a Fiber Bragg Grating (FBG) sensor. It consists of a periodic modulation of the refractive index of a short section of the core (< 1 cm). This particular "structure," obtained through laser photo inscription and called a Bragg grating, behaves like a frequency-selective mirror towards the light radiation passing through it. This means that all frequencies can pass through, except for a specific frequency that is reflected in the opposite direction: this, called the Bragg frequency, can be quantified in terms of wavelength as:

$$\lambda_B = 2n_{eff} \Lambda \quad (1)$$

Where  $n_{eff}$  is the average value of the refractive index of the core after the grating photo inscription, and  $\lambda_B$  is the grating pitch, which is the physical distance between two consecutive modulations. The value  $\lambda_B$  is exactly what is measured by the optical instrumentation and represents the sensor's response. Considering Eq. 1, it is immediate to understand how the wavelength reflected by the grating is proportional to the grating pitch, and therefore to a physical distance inherently related to the sensor's structure. Consequently, any physical parameter acting on the sensor will generate a variation in the reflected wavelength depending on the physical deformation applied to the sensor itself. Overall, therefore, indicating  $\varepsilon$  as a generic mechanical deformation induced by a generic load and  $T$  as the temperature acting on the sensor, it is possible to

write the general relationship that describes the behavior of an FBG sensor:

$$\Delta\lambda/\lambda = K_T \Delta T + K_\varepsilon \Delta\varepsilon \quad (2)$$

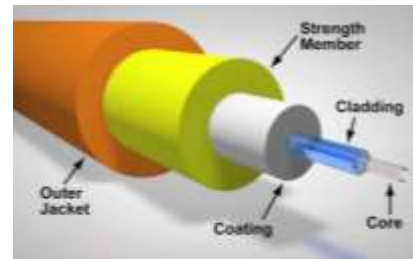


Figure 1. Optical fiber structure

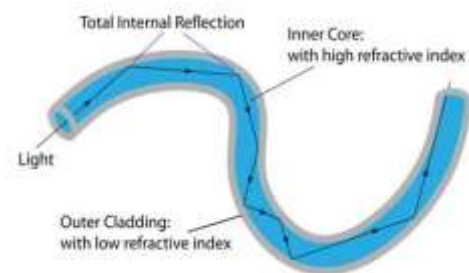


Figure 2. Optical fiber working principle

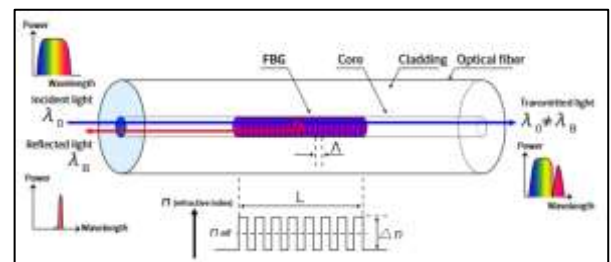


Figure 3. FBG sensor working principle

## 3 Physical set up

This study accounts for two specific calibration activities conducted in the laboratory regarding FBG optical sensing:

- Response to a thermal transient
- Response to mechanical vibration

The analysis of the response to a thermal transient described in this paper focuses on the third and final phase of a more complex test, which can be summarized by the following steps:

- Heating up to temperature
- Opening of the climatic chamber
- Closure of the climatic chamber

This report accounts for two specific calibration activities conducted in the laboratory regarding FBG optical sensing:

- Response to a thermal transient
- Response to mechanical vibration

The analysis of the response to a thermal transient described in this report focuses on the third and final

phase of a more complex test, which can be summarized by the following steps:

- Heating up to temperature
- Opening of the climatic chamber
- Closure of the climatic chamber

In the first two phases, the sensor response is influenced by convective air motions, creating a significant disturbance. In the third phase, however, heating occurs due to the heat transferred from the metallic supports of the experimental setup.

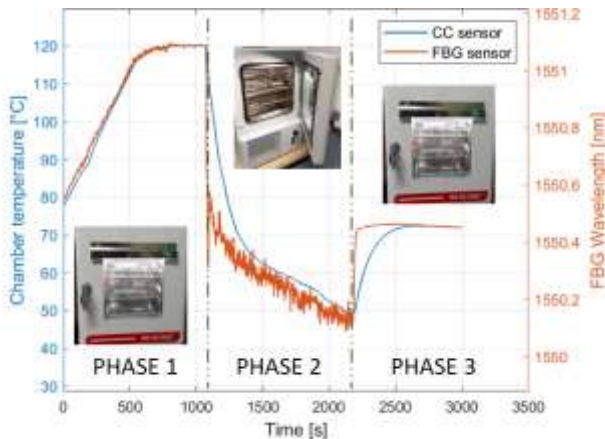


Figure 4. Physical thermal transient

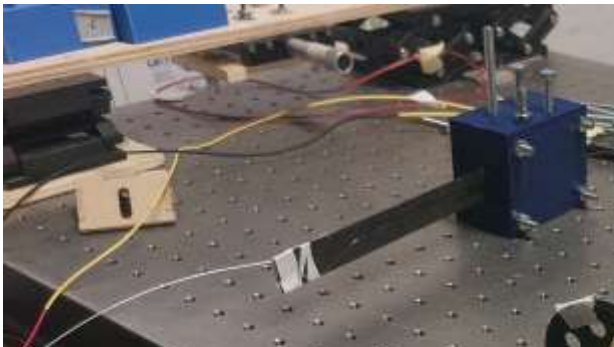


Figure 5. Physical mechanical load

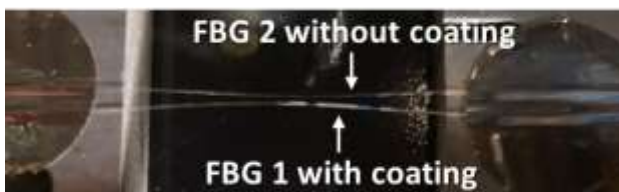


Figure 6. Optical fiber sensors

Consequently, the rising curve observed by the sensors is faithfully reproducible using a first-order model. Three sensors were involved in the study:

- FBG with the typical coating of optical fiber;
- FBG without the coating;
- PT100 electronic sensor.

Experimentally, a variation in sensor response time was observed depending on its configuration.

Through the first-order thermal model presented in this report, we aim to replicate the behavior of the three sensors by manipulating this parameter.

As for the mechanical activity, a carbon fiber laminate test piece was considered, onto which an optical fiber equipped with an FBG sensor was attached. This test piece, fixed at one end, is first deflected and then released, resulting in a damped vibration, typically describable with a second-order mass-spring-damper model. The experimental setup is completed by the optical data acquisition system, primarily consisting of the interrogator. This component can generate a light beam and send it into the fibers connected to it (via specific channels). Simultaneously, it can detect and quantify the wavelengths reflected by the FBGs, which are measured as sensor responses. The interrogator is connected to a PC via a LAN network cable through which it transfers the acquired data. Data management on the PC occurs in dual mode. On one hand, it is possible to monitor the instantaneous response of the sensor, displaying the sensor response as a "peak." On the other hand, the numerical values displayed on the monitor are saved to a text file. Acquisition can be performed at a sampling frequency ranging from 2.5 Hz to 2.5 kHz.

## 4 The proposed model

The described modeling can be divided into two main blocks:

- The thermal response of the sensors;
- The mechanical response of the sensor when subjected to a load induced vibration.

Regarding the thermal model, a typical first-order example was adopted. Considering the constitutive equation of the sensor and having arranged the optical sensor to be solely sensitive to temperature, it will output a value of  $\lambda$  directly proportional to the temperature variation. Mathematically, therefore, it is necessary to reproduce the purely thermal first-order model that describes the respective thermal transient, to which the conversion from temperature value to the one of wavelength reflected by the FBG grating must be added. Always starting from eq. (1), it is therefore easily obtainable.

$$d\lambda/dt = K_T dT/dt$$

The model can then be schematized into two parts:

- Thermal transient;
- Conversion of temperature into length.

The first part is exactly the one used in the course exercises for modeling the thermometer, of which the differential equation is reported for simplicity:

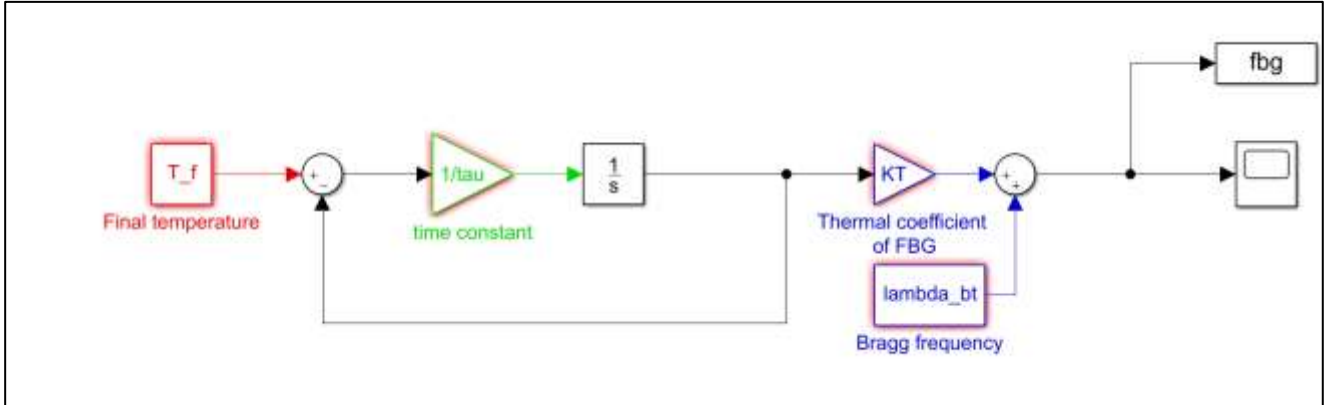


Figure 7. Optical fiber sensors

$$T_f = T_i + \tau \frac{dT}{dt} \quad (3)$$

In this part of the model, there are three parameters to input:

- Initial temperature;
- Final temperature;
- Gain.

Certainly, the most interesting aspect is represented by defining the value of the time constant  $\tau$ . Its value was derived from experimental data, considering the expression  $\tau=5\Delta t$ , where  $\Delta t$  is the total time duration of the transient. In the model, this parameter is incorporated into the gain, quantified as  $1/\tau$ .

The second part of the model, on the other hand, serves to convert the temperature data into the value of the wavelength reflected by the FBG sensor. It is represented solely by two blocks:

- A gain ( $K_T$ );
- A constant ( $\lambda_B$ ).

The gain  $K_T$  is directly the proportionality coefficient of the sensor obtained experimentally during the thermal calibration of the FBG grating.

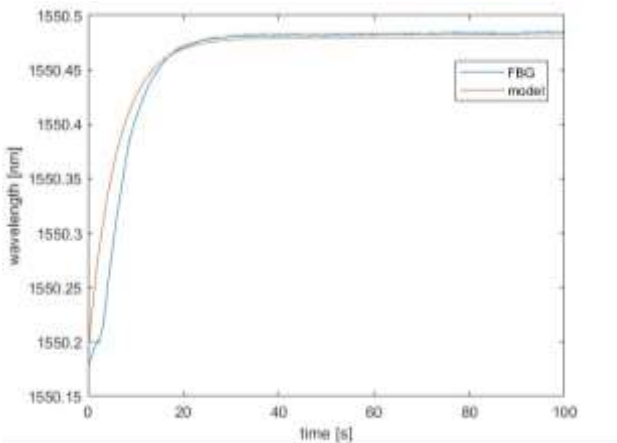


Figure 8. Comparison between thermal response of model and real FBG

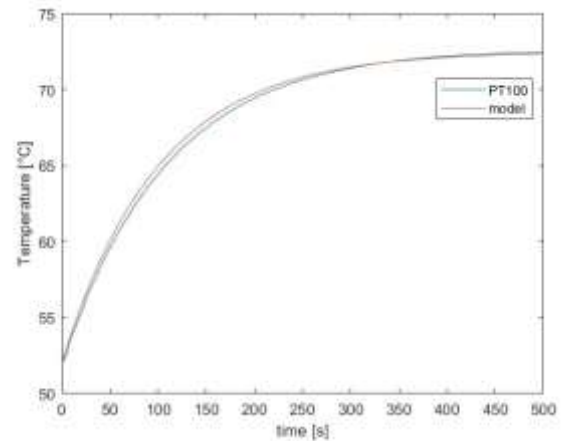


Figure 9. Comparison between model and real thermal PT100 sensor response

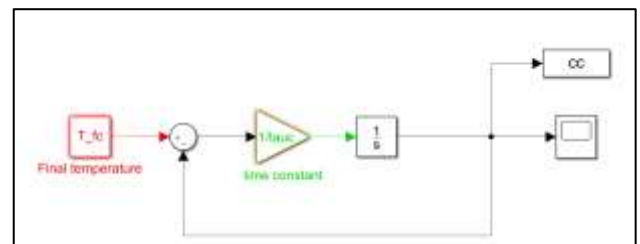


Figure 10. Optical fiber sensors

The constant, on the other hand, is the nominal value of the sensor provided under standard environmental conditions. The overall model is as shown in the figure, including the supporting MATLAB code employed. It can be observed that the model provides a good approximation of the sensor's response. However, in the initial phase of heating, there is a deviation from the typical first-order behavior of the experimental setup for a few seconds, leading to the

error depicted in the figure. As described in the previous section, the thermal responses of different sensor configurations were modeled to verify the different response times. In this regard, the comparison with the model for the environmental chamber sensor (PT100) is particularly significant. The approach is the same as in the previous case, but with variations in the characteristic response time. Since the PT100 is a much more stable thermal probe, the result provided by the model essentially coincides with the experimental data. Again, the model, MATLAB script, and comparison between responses are provided for reference. Finally, the same approach was repeated for the FBG sensor bonded to a carbon fiber specimen and subjected to a damped oscillation. In this case, the model is second order. The following model also consists of two main blocks:

- The mass-spring-damper model;
- The conversion of displacement along x into an optical value.

The model used is described by the following physical law:

$$(d^2 x)/(dt^2) = (F - Cdx/dt - Kx)/M \quad (4)$$

Therefore, the model includes the following parameters:

- Applied force to the system;
- Mass of the system;
- Stiffness;
- Damping.

In the second part of the model (in green), the following parameters appear:

- The proportionality coefficient between the displacement x and the optical value provided by the FBG grating,
- The nominal wavelength of the sensor.

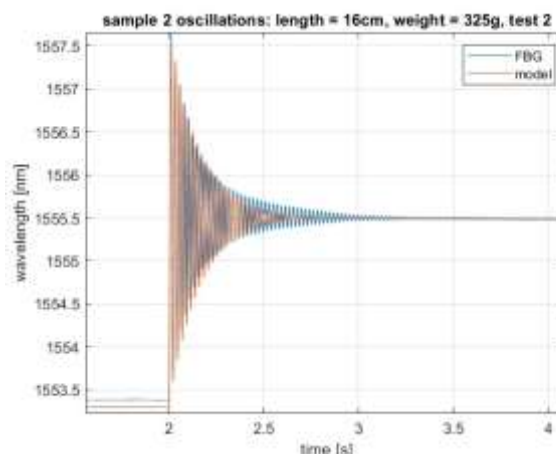


Figure 11. Comparison between mechanical response of model and real FBG

## 5. Conclusions

The article aims to provide a preliminary model of the response of FBG optical fiber sensors when used for monitoring aerospace systems. The results demonstrated good accuracy for the elementary case studies proposed, highlighting the possibility of numerically calculating the response of an FBG. In particular, the physical parameter conversion into a wavelength value through a constant gain has been validated. Moreover, considering the ability of grating to be sensitive to different physical parameters, it is possible to develop a numerical method for decoupling of thermal and mechanical effects on the sensor. However, to model more complex physical setups with adequate precision, the data highlights the need to increase the level of detail with which the phenomenon is modeled.

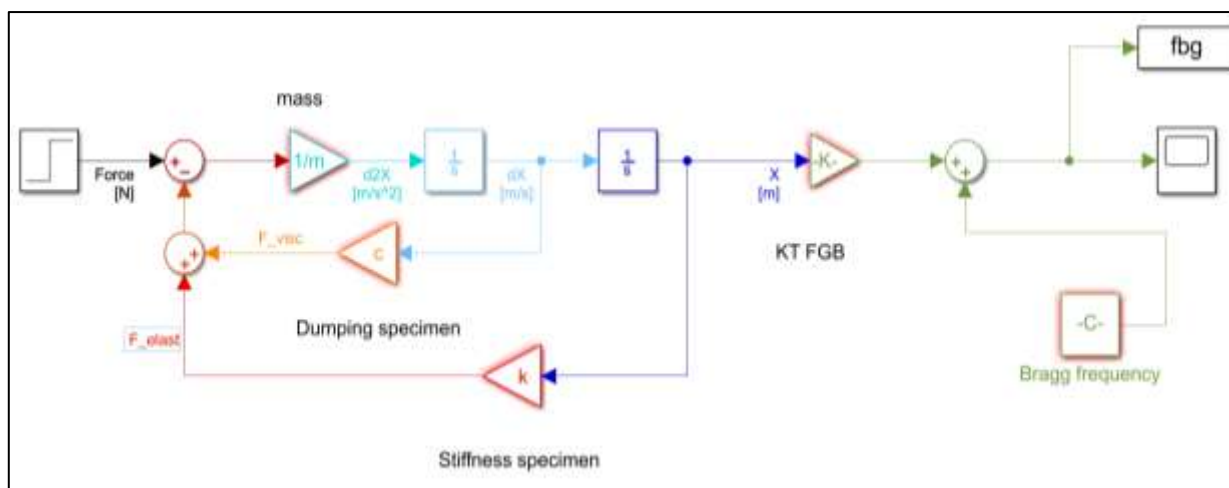


Figure 12. Optical fiber sensors

## References:

- [1] T. Missala, Electromechanical actuators – Selected safety-related problems, *Advances in Intelligent Systems and Computing*, vol. 267, pp. 175–186, 2014
- [2] A. Aimasso, Optical fiber sensor fusion for aerospace systems lifecycle management, *Materials Research Proceedings*, 2023.
- [3] Safa. Kasap, *Optoelectronics and photonics : principles and practices*, Prentice Hall, 2001.
- [4] G. P. Agrawal and S. Radic, Phase-Shifted Fiber Bragg Gratings and their Application for Wavelength Demultiplexing, *IEEE Photonics Technology Letters*, vol. 6, no. 8, pp. 995–997, 1994.
- [5] S. J. Mihailov et al., *Extreme Environment Sensing Using Femtosecond Laser-Inscribed Fiber Bragg Gratings*.
- [6] S. J. Mihailov, Fiber Bragg Grating Sensors for Harsh Environments, *Sensors*, vol. 12, pp. 1898–1918, 2012.
- [7] S. J. Mihailov et al., Ultrafast laser processing of optical fibers for sensing applications, *Sensors*, vol. 21, no. 4. MDPI AG, pp. 1–23, 2021.
- [8] H. Alemohammad, Opto-Mechanical Modeling of Fiber Bragg Grating Sensors, *Opto-Mechanical Fiber Optic Sensors: Research, Technology, and Applications in Mechanical Sensing*, Elsevier Inc., 2018, pp. 1–26.
- [9] R. Rodríguez-Garrido et al., High-temperature monitoring in central receiver concentrating solar power plants with femtosecond-laser inscribed fbg, *Sensors*, vol. 21, no. 11, Jun. 2021.
- [10] A. Behbahani, M. Pakmehr, and W. A. Stange, Optical Communications and Sensing for Avionics, *Springer Handbooks, Springer Science and Business Media Deutschland GmbH*, 2020, pp. 1125–1150.
- [11] L. Borello, G. Villero and M. D. L. Dalla Vedova, Flap failure and aircraft controllability: Developments in asymmetry monitoring techniques, *Journal of Mechanical Science and Technology*, 2014.
- [12] D. Belmonte, M. D. L. Dalla Vedova, and P. Maggiore, Prognostics of onboard electromechanical actuators: A new approach based on spectral analysis techniques, *International Review of Aerospace Engineering*, vol. 11, no. 3, pp. 96–103, 2018.

## Contribution of individual authors to the creation of a scientific article (ghostwriting policy)

Matteo D. L. Dalla Vedova and Alessandro Aimasso have implemented the proposed numerical model. Alessandro Aimasso and Matteo D. L. Dalla Vedova carried out the simulation and the optimization. Matteo Bertone and Alessandro Aimasso organized and executed the experiments of Section 4. Alessandro Aimasso cured the writing of the original draft and the visualization of results. Matteo D.L. Dalla Vedova and Paolo Maggiore were responsible for the critical analysis of the results obtained and supervised the review & editing of the final text.

## Sources of Funding for Research Presented in a Scientific Article or Scientific Article Itself

No funding was received for conducting this study.

## Conflict of Interest

The authors have no conflicts of interest to declare that are relevant to the content of this article.

## Creative Commons Attribution License 4.0 (Attribution 4.0 International, CC BY 4.0)

This article is published under the terms of the Creative Commons Attribution License 4.0

[https://creativecommons.org/licenses/by/4.0/deed.en\\_US](https://creativecommons.org/licenses/by/4.0/deed.en_US)